ELSEVIER

Marine Geology 183 (2002) 89–105

MARINE GEOLOGY
INTERNATIONAL JOURNAL OF MARINE GEOLOGY, GEOCHEMISTRY AND GEOPHYSICS

www.elsevier.com/locate/margeo

Microfabric study of diatomaceous and lithogenic deposition in laminated sediments from the Gotland Deep, Baltic Sea

Ian T. Burke, Ivailo Grigorov, Alan E.S. Kemp *

School of Ocean and Earth Science, University of Southampton, Southampton Oceanography Centre, European Way, Southampton SO14 3ZH, UK

Received 15 August 2000; accepted 28 August 2001

Abstract

The deep basins of the Baltic Sea are commonly anoxic, and finely laminated diatomaceous sediments have been deposited at intervals throughout the last 8000 yr. The origin and composition of individual laminae in Gotland Deep sediments have often proved difficult to characterise using traditional micropalaeontological and sedimentological studies. Here, we present a scanning electron microscope study in which lamina down to 30 μm in thickness with distinct mineralogical or micropalaeontological composition have been identified and described. Depositional laminae sequences in the form of couplets, triplets and quadruplets of diatomaceous and lithogenic laminae are observed with an average thickness of approximately 700 μm. Diagenetic Ca-rhodochrosite laminae also occur within these depositional sequences. Examination of the diatom assemblages suggests that these bundles of laminae represent annual deposits, or varves. Varves are relatively uncommon, and typically occur in small intervals of two to five varves, which are interrupted by more diffusely laminated and homogenous sediments. The origin of these more massive sediments probably relates to periodic re-oxygenation of the basin on inter-annual time scales and destruction of varves by bioturbation.

Keywords: laminated sediments; Baltic Sea; Littorina; diatoms; varves; microfabrics

1. Introduction

The Baltic Sea is a shallow enclosed basin, much of which is less than 50 m deep. There are a few isolated deep basins which include; the Gotland Deep (250 m), and the Bornholm Deep (80 m) (Fig. 1). The Baltic Sea drains a watershed more than four times its area, and there is limited exchange of saline North Sea water, producing the largest brackish water body in the world. As a result of this freshwater surplus, the Baltic Sea has a very strong salinity stratification in which a low salinity, well mixed, surface water layer (~2–8‰), is separated from more saline deep water (~11–15‰) by a permanent halocline at 60–80 m (Manheim, 1961; Kullenberg, 1981), which effectively restricts mixing of surface and deep waters (Matthäus, 1990). The deep basins and are only flushed during periodic saline inflows of North Sea water (Matthäus, 1995). Sedimentation below the halocline in the Gotland Deep is characterised by accumulation of fine grained organic-

* Corresponding author.
E-mail address: aesk@soc.soton.ac.uk (A.E.S. Kemp).

0025-3227/02/$ – see front matter
PII: S0025-3227(01)00250-X

carbon rich muds (Ignatius et al., 1981; Sohlenius, 1996), which have been intermittently laminated throughout the last ~8100 yr.

The laminated Gotland Deep sediments represent a good record of climatic and environmental changes affecting the entire Baltic Sea (Rahm, 1988). The origin and succession of lamina have proved difficult to describe using traditional diatom and sedimentological studies (Morris et al., 1988; Yemelyanov et al., 1995; Sohlenius and Westman, 1998). High-resolution SEM-based techniques using back-scattered electron images (BSE images) have been employed successfully to study laminated sediment fabrics in a wide range of other settings (e.g., Grimm, 1992; Kemp and Baldauf, 1993; Kemp, 1996; Pike and Kemp, 1996b; Pearce et al., 1998; Dean et al., 1999). Here, we present the results of a SEM-based microfabric study of the laminated Littorina sediments of the Gotland Deep.

1.1. Baltic stratigraphy

Since the onset of deglaciation, Baltic Sea stratigraphy has been controlled by the balance between global eustatic sea level rise and local isostatic uplift, leading to continual fluctuation of Baltic shorelines and connectivity to the World Ocean. The Late Pleistocene and Holocene (approx. 13 000 ^{14}C yr BP–present) history of the Baltic Sea and corresponding sediments are traditionally divided into the five stages summarised in Table 1.

2. Methods and materials

A 5.64 m gravity core, 20001-5, was collected in the Central Gotland Basin at 57°18.33′N, 20°03.00′E (Fig. 1), in a water depth of 243 m, during cruise 94.44.13.2 of R/V *Alexander Von Humboldt* in August 1994, as part of the Gotland Basin Experiment (GOBEX), (Emeis and Struck, 1998). Initial core description and sub-sampling was undertaken by staff of the Institute of Baltic Research at Warnemünde, Germany, where the core was sub-sampled into 25-cm wet sediment slabs and X-ray exposures were taken. The wet sediment slabs were vacuum packed in polythene bags to prevent desiccation. A radiocarbon ^{14}C-AMS age was obtained from a fish bone recovered from 205 cm in core 20001-5 for Dr. U. Struck (Institute of Baltic Research, Warnemünde), with a reservoir correction of −400 yr. Two kasten cores, 201301-5 and 201302-5, were also collected as part of GOBEX during cruise 4.3–13.3.96 of R/V *Poseidon* in February 1996, at 57°20.10′N, 19°57.50′E (water depth 237 m) and 57°15.14′N, 20°11.99′E (water depth 249 m) respectively. Preliminary fabric descriptions were prepared from X-ray images in Emeis and Struck (1998) for the post-Ancylus sections of 201301-5 and 201302-5, and are presented with logs for core 20001-5 in Fig. 2 only for reference purposes.

2.1. Sample preparation

Only material from core 20001-5 was prepared from SEM analysis. Sediment samples from two slabs, Slab 4 (71–93 cm) and Slab 6 (118–144 cm), shown on Fig. 2, were prepared for SEM study by embedding in epoxy resin using a fluid displacive impregnation technique modified from that described in Pike and Kemp (1996a) by Kemp et al. (1998). After partial desiccation during transit to the UK, Slab 4 showed signs of oxidation, and growths of gypsum crystals were observed on the sediment surface. The yellow Ca-rhodochrosite laminae were not evident in Slab 4, however, the sediment fabric was otherwise undisturbed, allowing examination of the primary sedimentary microstructure. In contrast, many yellow Ca-rhodochrosite were evident in Slab 6. Fluid displacive embedding allows thin section preparation with minimal fabric disturbance. Polished thin sections were prepared using an oil-based lubricant prior to fabric analysis carried out under the SEM.

2.2. Scanning electron microscopy

The polished thin sections were examined in the SEM using back-scattered electron (BSE) imagery. BSE images reveal the minerals, textures and fabrics of sediments and rocks in much greater detail than is possible with conventional optical microscopy (Krinsley et al., 1998). Back-scattered

Table 1
Stratigraphic stages of the Baltic Sea

Baltic stage[k] ^{14}C yr BP	Sediment type[a]	Organic carbon (wt%)[b]	Salinity (‰)[c]	Fossil assemblage	Environmental conditions
Baltic Ice Lake (~13–10.0 kyr BP)	Glaciogenic ice marginal varved clay	0.5	Fresh water	Sparse cold water diatoms[d]	Early ice-damned lake, formed from meltwater from the Weichselian Ice Sheet[f]
Yoldia Sea (10.0–9.5 kyr BP)	Glaciogenic microvarved clay	0.4	~10%	Brackish water diatoms and dwarf marine bivalve *Portlandia 'Yoldia' arctica*[e]	Formed after a catastrophic 25-m drop in lake level down to Yoldia sea level[g]. Brackish Conditions only persisted for 200–300 yr during mid Yoldia times[h,i]
Ancylus Lake (9.5–8.1 kyr BP)	Homogenous sulphide stained clay	1.2	Fresh water	Fresh water mollusc *Ancylus fluviatilis*[f]	Final lacustrine stage initiated by rapid isostatic uplift[f,g,h]
Littorina Sea (8.1–3 kyr BP)	Laminated and homogenous clay gyttja	3.0–5.5	25+	Brackish water diatoms[c]	Initiated by rapid eustatic sea level rise connection to the North Atlantic established the brackish conditions and salinity stratification that have persisted to the present day[c]. A 2 to 5% enrichment in manganese is due to the occurrence of rhodochrosite laminae[j]
Modern Baltic (3 kyr–present)	Mixed laminated and homogenous clay gyttja	3.0–5.5	6–9	Brackish water diatoms[c]	Continuation of Littorina stage, however slow isostatic uplift of sill region led to the restriction of saline inflow, reducing salinity[a,h]

[a] Ignatius et al., 1981.
[b] Danyushevskaya, 1992.
[c] Sohlenius et al., 1996.
[d] Kabailiené, 1995.
[e] Raukas, 1995.
[f] Zenkevitch, 1963.
[g] Björck, 1995.
[h] Mörner, 1995.
[i] Wastegård et al., 1995.
[j] Huckriede and Meischner, 1996.
[k] Björck et al., 1996.

electrons undergo elastic collisions and are subsequently directed back out of the sample. The ratio of back-scattered/incident electrons defines the back-scattering coefficient (η) which is a function of the atomic number of the sample. Thus, for highly polished flat specimens, the brightness within the BSE image is proportional to the atomic number of the sample. Minerals with high mean atomic number such as pyrite ($\eta = 0.247$) are very bright (see Fig. 5B) while those with intermediate mean atomic number such as dolomite ($\eta = 0.133$) are mid grey (see Fig. 5A) and the epoxy resin is black (Krinsley et al., 1998). Since the epoxy resin has been absorbed into all pore spaces in the sediment, the overall distribution of brightness or darkness within an image is effectively a porosity map of the specimen. In lower magnification images (e.g. Fig. 7) the less porous clay-rich sediment laminae stand out from the darker diatomaceous laminae, in which the resin has pervasively entered the more open diatom framework. To complement BSE imagery, semi-quantitative, non-destructive energy dispersive X-ray microanalysis (EDS) was also undertaken and X-ray diffraction analysis was undertaken on representative intervals to aid mineral characterisation (see Fig. 3).

Counterparts of the sediment prepared as polished thin sections were broken off, dried, mounted on stubs and examined under SEM to produce topographic BSE images (analogous to secondary electron images) to aid identification of microfossils, mineral habits and sediment fabrics (see Fig. 4).

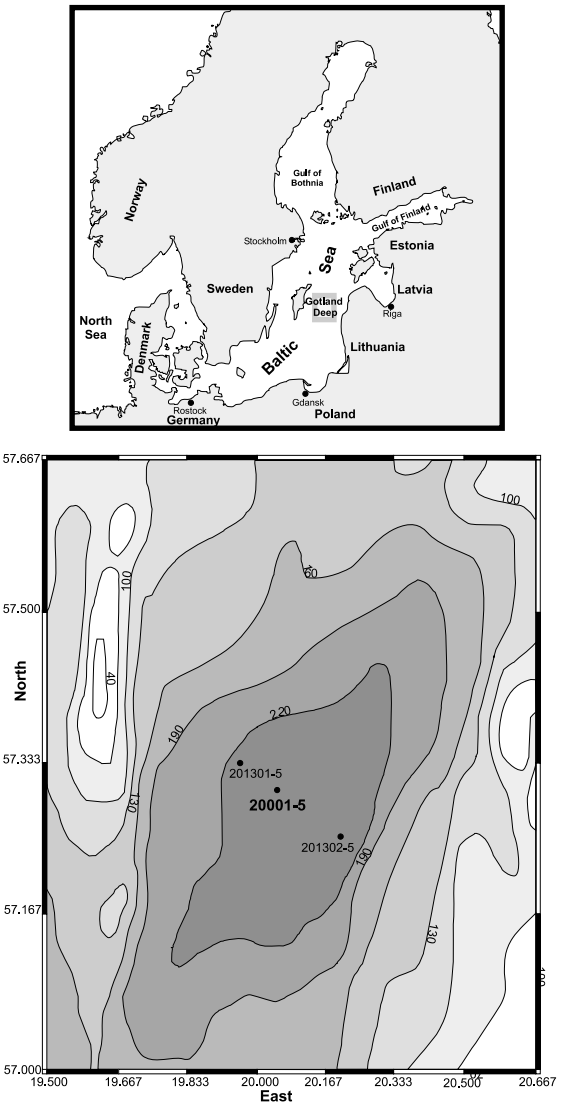

Fig. 1. Map of Baltic Sea, bathymetry of the Gotland Basin (after Emeis and Struck, 1998), and core location for 20001-5, 201301-5, and 201302-5.

3. Results

3.1. Fabric description

Laminated sediments occur in core 20001-5 from the Ancylus–Littorina boundary at 229 cm upwards throughout most of the core (Fig. 2). There are two intervals of homogenous, bioturbated sediments in the lower Littorina section, from 143–166 cm and from 182–194 cm. The remaining laminated sediments contain relatively thin (1–3 cm) well-laminated intervals interbedded with thicker intervals of indistinctly laminated sediments. The Modern Baltic sediments, which occur from 0 to 66 cm, are characterised by mixed packets of laminated and homogenous sediments. There are at least six occurrences of macro-scale erosional features observable within the post-Ancylus muds, where laminations are clearly truncated. The fine scale sediment fabric becomes apparent upon examination of low mag-

nification (×5) BSEI base maps. Laminae observed in Slab 6 are presented in Table 2 and can be divided into six main lamina types. The same lamina types were observed in Slab 4, with the exception of Ca-rhodochrosite laminae which were absent.

3.2. Mineral composition

XRD analysis was performed on five representative 1-cm intervals from Slab 6 in order to determine general mineral composition: (1) well-laminated mud; (2) mixed laminated and homogenous mud; (3) homogenous mud; (4) well-laminated mud with visible yellow Ca-rhodochrosite laminae; (5) homogenous mud, with visible yellow Ca-rhodochrosite laminae. All XRD traces show peaks representing the primary clastic minerals, quartz, illite, and plagioclase feldspar, and kaolinite, with smectite present in samples 1–3. This is typical of Gotland Deep mineral assemblages (Gingele and Leipe, 1997). Ca-rhodochrosite was determined in samples 4 and 5 by comparison to XRD traces presented in Heiser et al. (2001). Peaks representing gypsum occurred in samples 1–3 and 5. The occurrence of gypsum is most likely to relate to oxidation in transit (Section 2.1), and not to primary sedimentation or diagenetic processes.

3.3. Diatomaceous laminae

In thin section, diatomaceous material can easily be recognised in BSE images due to their distinctive shapes, although identification to species level is only possible in three dimensional topographic BSE images. EDS spot analysis of diatom frustules produced compositions rich in Si and O, as expected for opaline silica. Diatomaceous laminae may be sub-divided on the basis of diatom content into two distinct lamina types.

3.3.1. Diatom ooze laminae (>80% diatom frustules)

Diatom ooze laminae contain mixed species assemblages or less commonly near-monospecific oozes of *Thalassionema nitzschioides* (Fig. 5b) or of *Pseudosolenia calcar-avis* frustules. While *T. nitzschioides* frustules are still intact, *P. calcar-avis* girdle bands are always separated (Fig. 4B). The diatom frustules appear to be well preserved and even lightly silicified rhizosolenid girdle bands are observed intact. Diatom identification to species level in *P. calcar-avis* deposits is only possible where a high density of terminal processes can be observed. Laminae of *T. nitzschioides* are usually very thick (300–600 μm), in contrast laminae of *P. calcar-avis* are usually much thinner (100–200 μm). *Chaetoceros* spp. resting spores also form ooze deposits, but are rarely monospecific. The resting spores of *Chaetoceros lorenzianus* and *Chaetoceros diadema* were found to co-occur with *T. nitzschioides* (Fig. 4D). Other *Chaetoceros* spp. resting spores formed minor constituents, but were observed rarely. There is no apparent vertical succession between the *C. lorenzianus* and *C. diadema* resting spores. The weakly silicified *Chaetoceros* spp. vegetative cells are very rarely

Table 2
Lamina type descriptions, Core 20001-5, Slab 6, 118–144 cm

Lamina type	Number of occurrences	Thickness range (μm)	Average thickness (μm)	Description
Diatom ooze	82	<100–1800	325	More than 80% diatom frustules, mono-specific or mixed diatom assemblage
Diatomaceous mud	198	200–800	380	Diatom-rich, 50–80% diatom frustules, mixed assemblage
Clay-rich mud	165	150–1000	425	More than 50% clay matrix, minor diatom assemblage
Barren mud	64	100–2900	600	More than 90% clay matrix
Silt-rich mud	30	50–150	90	Clay-rich matrix with more than 20% silt grains
Ca-rhodochrosite	95	<80–350	135	Dense aggregates of distinctively bright crystals

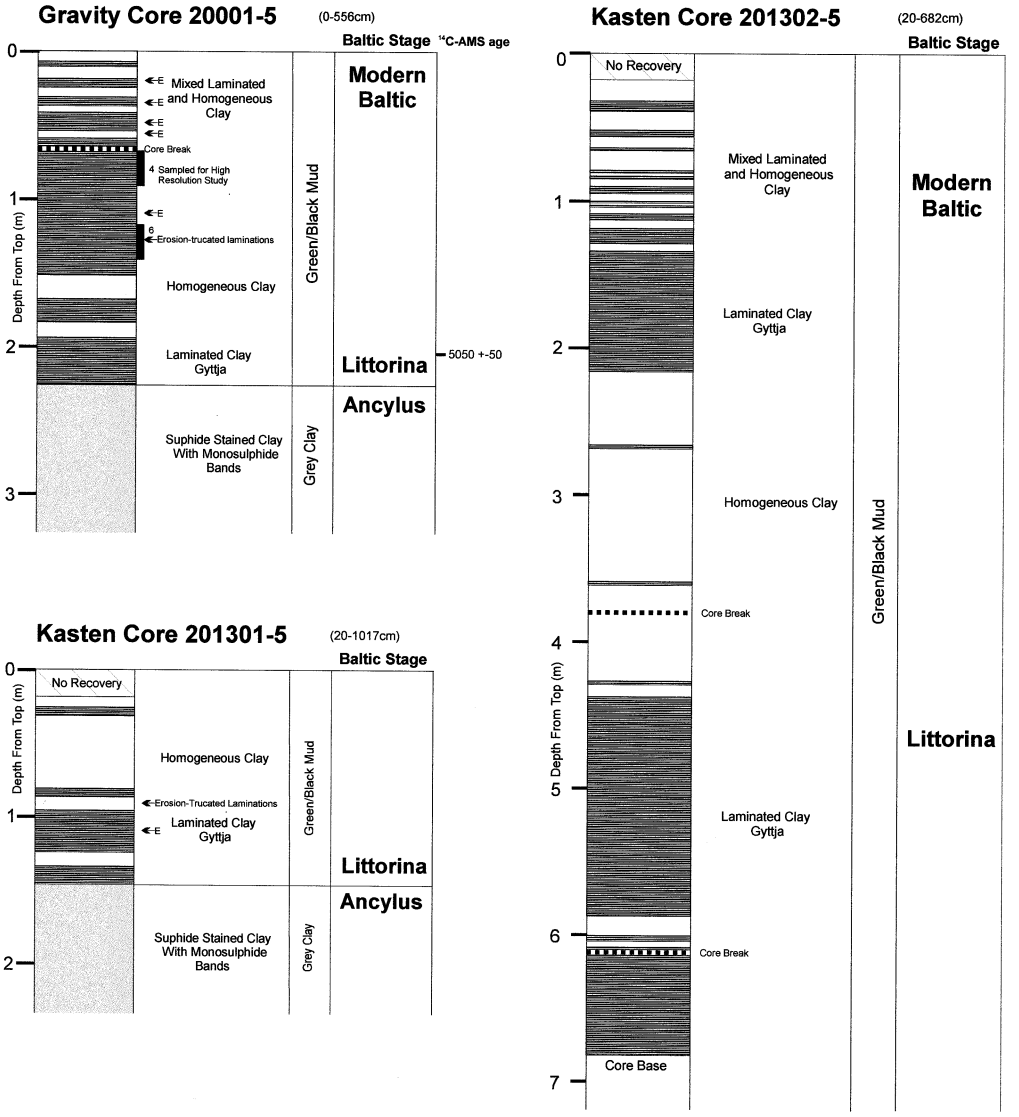

Fig. 2. Lithology and stratigraphy of cores 20001-5, 201301-5 and 21302-5, Intervals sub-sampled for high resolution study marked by black rectangles. Logged from X-ray images in Emeis and Struck (1998) by I.T. Burke

present. Small centric (<50 μm) *Thalassiosira* spp. frustules (Fig. 4E), also occur in *Chaetoceros* spp. oozes. The frustules are well preserved, with no signs of dissolution, and are rarely broken.

3.3.2. Diatomaceous mud laminae (50–80% diatom frustules)

Diatomaceous muds most commonly contain mixed *Chaetoceros* spp. resting spores (Fig. 5C), although rhizosolenids and chrysophyte cysts (Fig. 4C) can also be present. Again there is no apparent vertical succession, commonly two or more species of variable abundance are mixed homogeneously. Occasionally up to five species are found in diatomaceous mud laminae. There is commonly a progressive increase in the propor-

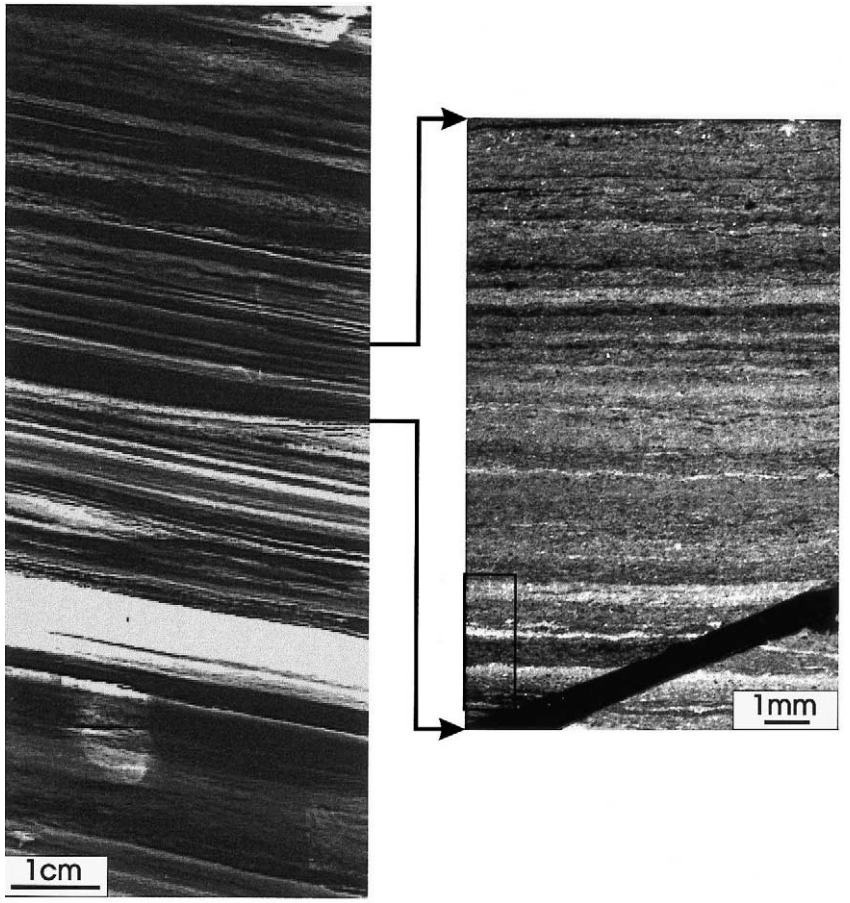

Fig. 3. X-ray exposure of core 20001-5, 118–128 cm (left), and low resolution ×5 BSE image of typical laminated section (right). Box shows position of ×75 BSE image shown in Fig. 6A.

tion of clay material present towards the lamina top.

3.4. Lithogenic laminae

In most BSE images the most common material observed consist of aggregates of very small (less than 2 μm) crystals, which create a grey background in many images. No distinct crystal shapes are evident, however, EDS spot analysis of this material revealed that it was composed largely of Al, Si, and O, with variable minor amounts Fe, Mg, K, Na and Ca, and was inferred to represent the clay minerals determined by XRD. Separate feldspar grains where not observed by EDS spot analysis and may form part of the fine background matrix. In this study the term 'silt' simply refers to any clastic mineral grain larger than 2 μm. Silt grains are commonly irregular and angular in BSE images, and Si- and O-rich (quartz, centre Fig. 5D), and Ca-, Mg-, C- and O-rich (dolomite, centre Fig. 5A) grains, were the two main types determined by EDS spot analysis. All clay-rich laminae are usually massive, with no apparent grain size grading and pellets are very rarely observed. Clay-rich laminae may be divided in three distinct types based on the dominance of clay matrix, diatom, and silt content.

3.4.1. Clay-rich mud laminae (50–90% clay matrix)

Clay-rich mud laminae commonly contain the

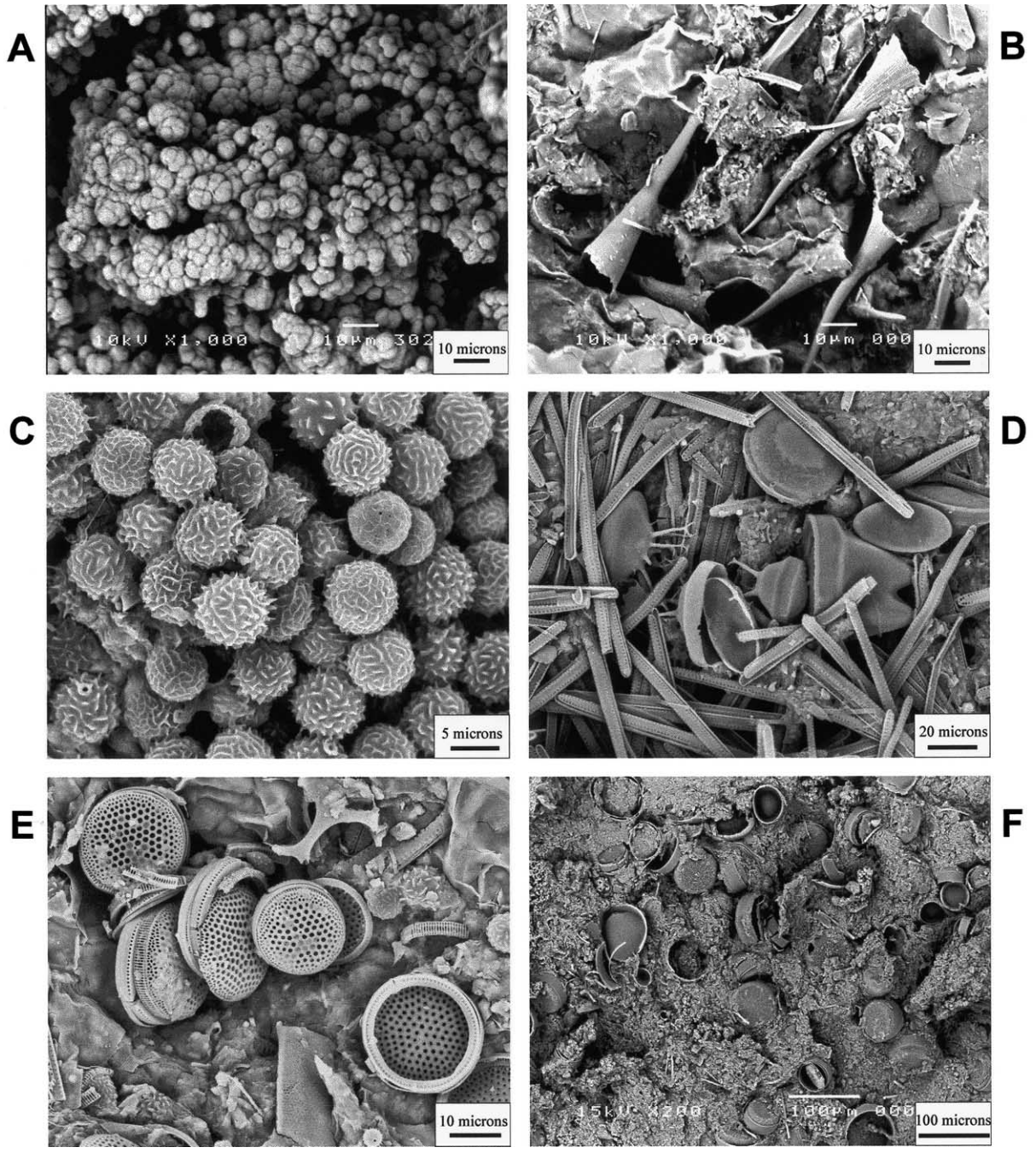

Fig. 4. High magnification topographic BSE images. (A) Aggregate of rhodochrosite crystals. (B) Intact terminal processes of *Pseudosolenia calcar-avis*, with disjointed girdle bands. (C) Chrysophyte cysts. (D) Mixed assemblage ooze with, *Thalassionema nitzschioides*, *Chaetoceros lorenzianus* and *Chaetoceros diadema*. (E) *Thalassiosira* spp. frustules. (F) Diatomaceous mud with *Actinocyclus* spp. frustules.

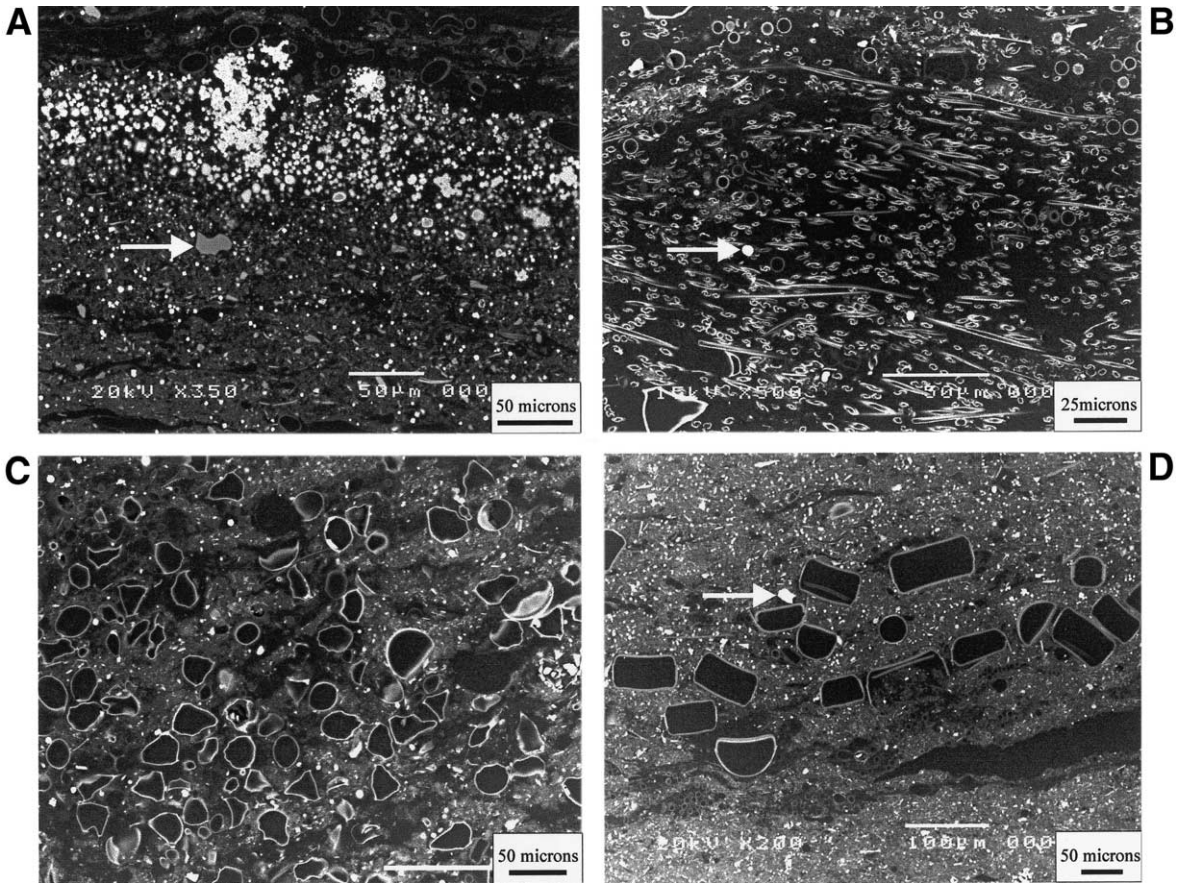

Fig. 5. High magnification BSE images. (A) Bright rhodochrosite lamina, between Clay-rich mud and ooze lamina. Dolomite grain marked by white arrow. (B) Pennate diatom ooze lamina, most likely to be *Thalassionema nitzschiodes*. Framboidal Fe-sulphide grain marked by white arrow. (C) Mixed *Chaetoceros* spp. mud lamina. (D) Terrigenous mud lamina with large centrics. Quartz grain marked by white arrow.

large centric diatom (greater than 50 μm) *Actinocyclus* spp. (Figs. 4F and 5D), either distributed evenly throughout the lamina or as a continuous sub-lamina. Often small amounts of *Chaetoceros* spp. resting spores and chrysophyte cysts are also observed within clay-rich laminae. There is commonly an upward increase in the amount of clay material present towards the lamina top.

3.4.2. Barren mud laminae (>90% clay matrix)

These are distinguished from clay-rich mud laminae by very low diatom content.

3.4.3. Silt-rich laminae

Distinct, thin (50–150 μm) silt-rich mud laminae occur irregularly and infrequently with a >20% silt fraction.

3.5. Diagenetic minerals and laminae

3.5.1. Ca-rhodochrosite laminae

Diagenetic Ca-rhodochrosite laminae occur regularly throughout the Littorina sediments of the Gotland Deep. Ca-rhodochrosite laminae contain aggregates of 2–10 μm globular crystallites (Fig. 4A), which in BSEI appear as bright rounded, often hollow grains (Fig. 5A). Ca-rhodochrosite crystallites are also occasionally observed as overgrowths on detrital dolomite grains or encrusting benthic foraminifera tests, but are not observed to

encrust diatom frustules. There is normally large thickness variation within individual Ca-rhodochrosite laminae, and dense nodular aggregates may occur both within Ca-rhodochrosite laminae, and in isolation within other laminae.

In well-laminated Ca-rhodochrosite laminae usually have well defined upper and lower transitions, but within the more massive intervals Ca-rhodochrosite may occur in dispersed bands, (although individual Ca-rhodochrosite laminae can be still distinguished). In some cases, Ca-rhodochrosite crystallites appear to distributed across the contact between other laminae (e.g. Fig. 6A). Rare tests of the benthic foraminifera, *Elphidium excavatum* (Terquem), *Elphidium albiumbilicatum* (Weiss), *Ammonia* sp., *Spiroloculina canaliculata* (d'Orbigny) and *Cassidulina* sp., are found encrusted in Ca-rhodochrosite, associated with rho-

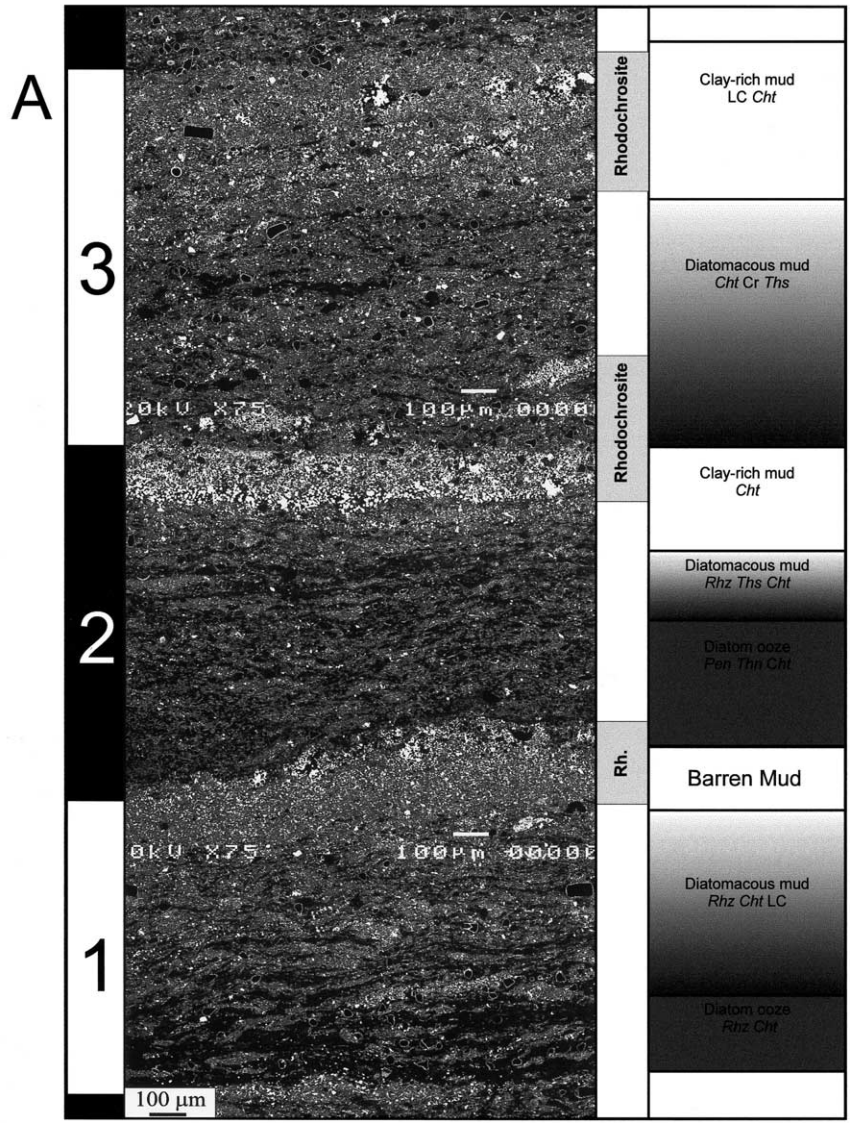

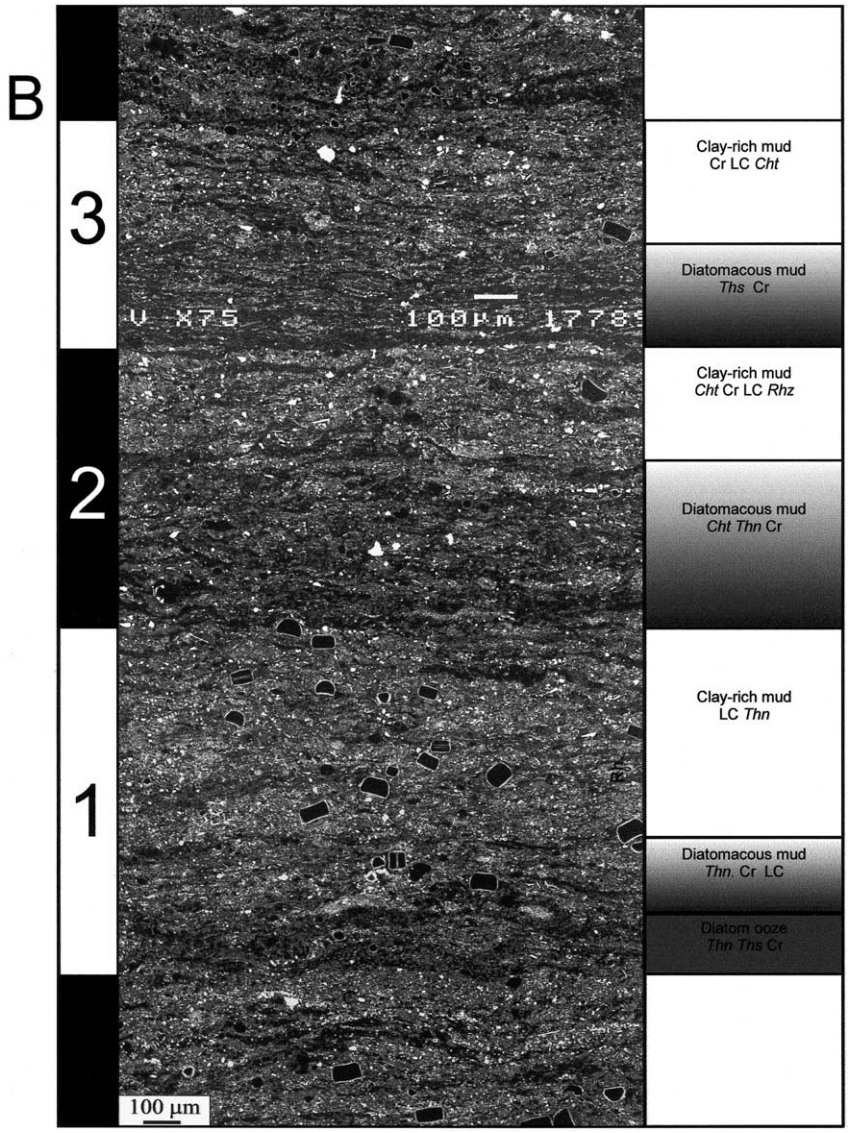

Fig. 6. (A) ×75 BSE image mosaic from Slab 6 (core depth 126 cm) (B) ×75 BSE image mosaic from Slab 4 (core depth 77 cm). Both sections show three depositional sequences (1–3), and are shown with descriptions of laminae composition. Although there is considerable variation in the precise lamina make-up between depositional sequences, these cycles are proposed to represent annual deposition, i.e. varves. LC = large centrics, Cht = *Chaetoceros* spp. resting spores, Cr = Chrysophyte cysts, Ths = *Thalassiosira* spp., Thn = *Thalassionema* spp., Rhz = rhizosolenids.

dochrosite laminae. For a full discussion of Ca-rhodochrosite formation mechanisms in the Gotland Deep see Huckriede and Meischner (1996), Sohlenius et al. (1996), Neumann et al., (1997) and Sternbeck and Sohlenius (1997).

3.5.2. *Fe-sulphides*

The very brightest individual grains in BSE images, when determined by EDS spot analysis were found to be rich in Fe and S, and inferred to represent Fe-sulphides. Small (2–10 µm) Fe-sul-

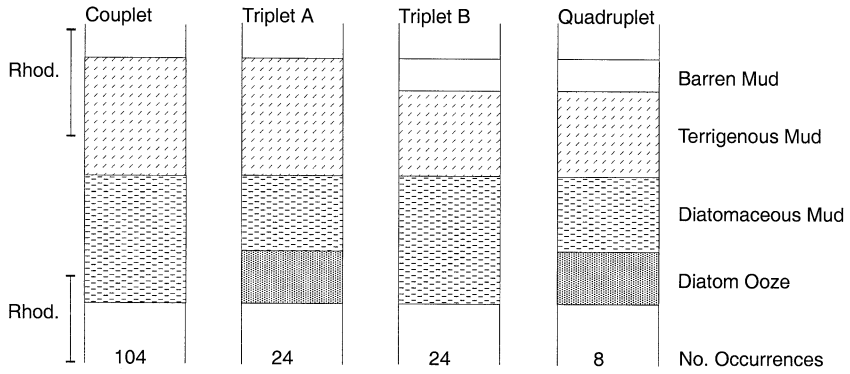

Fig. 7. The different lamina sequences, or varves, found in Gotland Deep sediments, including numbers of occurrences. Observed position of Ca-rhodochrosite lamina in varves is also denoted.

phide crystallites were observed to occur in both rounded framboidal (e.g. centre Fig. 5B) and cubic forms (e.g. dispersed below Ca-rhodochrosite laminae Fig. 5A). Fe-sulphides do not from distinct laminae, rather they occur finely dispersed more or less continually throughout all laminae in the section. See Boesen and Postma (1988), Neumann et al. (1997) and Sternbeck and Sohlenius (1997) for detailed discussion of Fe-sulphide formation in the Gotland Deep.

3.6. Succession of laminae

Throughout the laminated sections of Slab 4 and Slab 6 there are short 1–4-mm intervals containing distinct diatomaceous and clay-rich laminae, intercalated with intervals of indistinct laminae or massive sediment. Fig. 6 shows examples of two such intervals, one containing (Fig. 6A), and one without Ca-rhodochrosite laminae (Fig. 6B). Most commonly laminae are organised in simple couplets of alternating diatomaceous mud laminae and clay-rich mud laminae, but triplets and occasionally quadruplets are also observed, defined by the presence of additional distinct diatom ooze or barren mud laminae (Fig. 7). A common feature of these couplets, triplets and quadruplets is an increase in clay material upward at the expense of diatom content, as can be seen clearly for sequence A1 in Fig. 6. Thus, when distinct diatom ooze laminae occur they are present at the base of the sequence, and conversely when barren muds occur they are at the top. The upper boundaries of clay-rich laminae are commonly well defined. Ca-rhodochrosite laminae occur in A1–3 (Fig. 6A). Of the 95 Ca-rhodochrosite laminae occurrences in Slab 6 (Table 2), 31 are within recognisable couplets, triplets or quadruplets. Ca-rhodochrosite laminae always occur towards the top part of the clay-rich mud laminae or between the clay-rich laminae and the following diatomaceous laminae.

Fig. 7 shows the abundance of couplets, triplets and quadruplets observed in Slab 4 and Slab 6. Simple couplets of diatomaceous mud laminae and clay-rich mud laminae are most common, accounting for 104 sequences. Triplets make up 48 sequences. There are 24 occurrences each of the simple couplet plus an extra basal diatom ooze lamina generally of *Thalassionema nitzschioides* and *Chaetoceros* spp. resting spores (Triplet A) or an extra upper barren mud laminae (Triplet B). Only eight quadruplets containing four separate laminae are observed. A total of 160 couplets, triplets and quadruplets were observed in Slab 4 (103) and in Slab 6 (57). The average thickness of these groups of laminae in Slab 4 and Slab 6 is approx. 680 μm, and 750 μm, respectively, producing an overall average thickness of approx. 700 μm. In Slab 4 and Slab 6 these depositional sequences account for approx. 16% and 31% of the record, respectively, and typically only two to five groups of laminae occur continuously in any one section.

4. Discussion

4.1. Diatom palaeoecology and occurrence in the annual sedimentation cycle

The diatom assemblages observed in this study are distinctly different from those described in modern Baltic assemblages. This is possibly due to changes to Baltic environmental conditions since Littorina times (Sohlenius et al., 1996), and the effects of silica dissolution which can modify the species composition occurring in the water column when compared to that preserved in the sediments (Sancetta, 1989; Heiskanen and Kononen, 1994). There is a large surface water salinity difference between modern Baltic conditions, 2–8‰, and Littorina conditions of up to 20‰ (Sohlenius et al., 1996). Therefore, salinity sensitive species like *Pseudosolenia calcar-avis calcar-avis*, which is common throughout Littorina sediments (Yemelyanov et al., 1995), are not present in modern Baltic water column and sediment assemblages (Zenkevitch, 1963; Hallfors et al., 1981; Morris et al., 1988; Jansson, 1989; Heiskanen and Kononen, 1994). Also, *Chaetoceros* spp. resting spores are very common within Littorina sediments, but the delicate vegetative cells and setae are very rarely observed. It is therefore possible for lightly silicified species, which do not employ a well-silicified stage in their life cycle, to be missing from the record.

The palaeoecology of Baltic Littorina diatom assemblages may be inferred from numerous other studies of either modern or fossil assemblages.

Mixed diatomaceous laminae, containing *Chaetoceros lorenzianus* and *Chaetoceros diadema* resting spores, *Thalassiosira* spp. and *Thalassionema nitzschioides* are common in Littorina sediments. A common feature of these species is their small size, typical of rapid growing diatoms in spring blooms or upwelling pulses (Margalef, 1967; Kemp et al., 2000). The fabric of the deposits also suggests that the assemblages were formed and sedimented out of the water column rapidly before grazing could break the frustules (Fig. 4D,E). In the Littorina sediments these diatomaceous laminae are thought to represent rapid sedimentation from diatom spring blooms.

Following the water column studies by Alldredge and Gotschalk (1989) aggregation of *Chaetoceros* spp. blooms, Grimm et al. (1996) ascribed large concentrations of *Chaetoceros* spp. resting spores in sediment laminae to 'self sedimentation' at the end of bloom events. Bull and Kemp (1995) also attribute the formation of *Chaetoceros*-rich deposits to the mass flocculation of *Chaetoceros* spp. resting spores following bloom events. While *Chaetoceros lorenzianus* and *Chaetoceros diadema* resting spores very often co-occur in diatom ooze or diatomaceous laminae, there is some uncertainty about the overlap between each species ecological requirements, as inferred from modern assemblage studies. Canonical correspondence analysis of Saanich Inlet, British Columbia, laminated sediments suggest that *C. lorenzianus* has low temperature and high salinity optima (McQuoid and Hobson, 1997). In Narragansett Bay, Rhode Island, *C. diadema* is commonly found in early spring and rarely in the autumn (Rines and Hargraves, 1988). *Thalassiosira* spp. typical of northern, cold water regions are often found in early spring diatom water column assemblages (Morris et al., 1988; McQuoid and Hobson, 1997; Pike and Kemp, 1997). *Thalassionema nitzschioides* is most abundant in late spring/early summer water column assemblages (McQuoid and Hobson, 1997), and *T. nitzschioides* is commonly found as a component of a mixed assemblage ooze with *Chaetoceros* spp. in other settings (Brodie and Kemp, 1994; Bull and Kemp, 1995; Pearce et al., 1998).

Chrysophyte cysts are typically found in the upper part of diatomaceous mud laminae or within clay-rich laminae, and are reported to bloom in great abundance during early summer in the Baltic Sea (Hallfors et al., 1981).

Thin laminae of *Pseudosolenia calcar-avis* ooze are occasionally observed with an irregular occurrence. These near-monospecific ooze laminae are thought to form by rapid diatom deposition following disruption of stratification in autumn/early winter. In contrast to the 'spring bloom' species, *P. calcar-avis* is slow growing (Guillard and Kilham, 1978) and adapted to stratified, oligotrophic conditions, yet recent studies have shown that it may be a major component of flux to the sea

floor. Many rhizosolenids can regulate their buoyancy to retrieve nutrients from the thermocline/nutricline (Villareal et al., 1993), and may occur in positively buoyant macroscopic aggregates up to 30 cm in size (Villareal and Carpenter, 1989). Sediment-trap time series study off the coast of Oregon, showed maximum *P. calcar-avis* fluxes during late fall and winter in three consecutive years (Sancetta et al., 1991). Kemp et al. (1999) have also reported near-monospecific *P. calcar-avis* ooze laminae in Mediterranean sapropels, which are attributed to late autumn/early winter flux events. In a new synthesis of diatom flux observations from laminae and from sediment traps, Kemp et al. (2000) attribute such flux events to break down of the summer thermocline and rapid deposition of the rhizosolenid diatoms in an autumn or 'fall dump' (Smetacek, 2000).

Clay-rich laminae containing *Actinocyclus* spp. are commonly found following the spring/summer diatomaceous laminae. Although not identified to species level in this study, Sohlenius et al. (1996) found that *Actinocyclus octonarius* and *Actinocyclus ehrenbergii* are the most common in Gotland Deep Littorina sediments. These species commonly occur in brackish–marine environments (Guillard and Kilham, 1978). The genus is typically epiphytic on seaweed but is a common constituent of the nearshore plankton (Round et al., 1990). In modern central Baltic assemblages, *A. octonarius* are most abundant in late summer to early autumn (Hallfors et al., 1981).

4.2. Terrigenous sedimentation

Although the ultimate source of the clay material found in Gotland Deep sediments is considered to be terrestrial deposits, the main direct source of terrigenous clays to the Gotland Deep is from erosion and resuspension of coastal and shallow water sediments during storms (Gingele and Leipe, 1997), or by bottom erosion due to saline inflows (Sviridov et al., 1997; Emeis et al., 1998; Sivkov et al., 1998). Both storm erosion and saline inflows are distinctly seasonal and are maximised in winter (Matthäus and Schinke, 1994; Matthäus, 1995). Bergstrom and Carlsson (1994) and Schinke and Matthäus (1998) also report that river runoff peaks in winter in many years, but river sediment input is generally small and is initially deposited only in shallow water, and is likely to go through several resuspension and deposition events before finally being deposited the deep basins (Gingele and Leipe, 1997). The neritic diatom species *Actinocyclus* spp. which commonly occur in clay-rich laminae, are therefore, inferred to be redeposited in the Gotland Deep simultaneously with this reworked terrigenous material.

4.3. Annual succession and varves

The couplet of diatomaceous mud and clay-rich mud commonly observed in the Gotland Deep sediment is typical of the annual biogenic–lithogenic sedimentation couplets or varves found in marine settings adjacent to land (e.g. Sancetta, 1996). The diatom component forms during the spring–summer growing season while the terrigenous sediment input is dominant in winter when biogenic production is minimal and storms redistribute sediment to the basin. The triplets and quadruplets in which purer diatom ooze or mud 'end-member' laminae may be identified are also consistent with annual sedimentation cycle (Figs. 6 and 7).

Fig. 6 shows examples of six lamina sequences, that form couplet or triplet varves. Sequences A1, A2, A3, B1 and B2, have a well defined start and finish and an upward transition from a diatomaceous mud or ooze lamina to a clay-rich lamina. The diatomaceous laminae in each sequence contain diatom species typical of sedimentation following spring/summer blooms, such as *Thalassiosira* spp., *Thalassionema nitzschioides*, smaller *Chaetoceros* spp. resting spores and chrysophyte cysts. The clay-rich lamina of each sequence contains only sparse assemblages of larger diatoms typical of autumnal production. Sequence B3 also contains a two-lamina sequence with a diatom succession typical of annual production, however, the upper boundary is somewhat transitional.

The concentrations of Ca-rhodochrosite observed within lamina sequences only occur in the upper part of winter clay-rich mud laminae or just

encroaching on spring diatomaceous mud laminae (e.g. Fig. 6A1–3), and therefore, in this context represent an exclusively winter/early spring phenomenon.

4.4. Sedimentation rates

In previous Baltic Sea studies the arguments in favour of the existence of varves have also been based on the relationship between laminae couplet thickness and radiochemical (Jonsson, 1992; Salonen et al., 1995) and bulk (Ignatius, 1958) sedimentation rates. If the depositional sequences do indeed represent varves, then this is problematic in terms of sedimentation rates with respect to the thickness of post-Ancylus sediments in core 20001-5. The post-Ancylus sediments in the Gotland Deep represent approximately 8100 yr. The measured varve thickness of approximately 0.7 mm would imply approximately 5.7 m of deposition. Core 20001-5, however, only contains 2.29 m of post-Ancylus sediments, implying a sedimentation rate of only 0.28 mm per year. This discrepancy may be explained by either or both of the following: (1) The sedimentation rate indicated by varve thickness is not typical of the core as a whole, and varve sequences represent periods of more rapid sedimentation; and/or (2) Core 20001-5 has been significantly eroded.

The post-Ancylus sediment thickness is asymmetrical from the NW to the SE across the Gotland Deep, and reported mean sedimentation rate varies from 0.23 to 0.75 mm per year (Christiansen and Kunzendorf, 1998). This can be clearly seen in the three cores, presented in Fig. 2; 201301-5, 20001-5 and 201302-5. The Ancylus–Littorina boundary is not observed in core 201302-5 before the core base at 6.82 m, implying an average sedimentation rate in excess of 0.85 mm per year. This asymmetry in sedimentation is attributed to bottom erosion by the periodic inflows of North Sea water into to the Baltic (Emeis et al., 1998; Sivkov et al., 1998). In addition, Sviridov et al. (1997) have observed erosional bottom features that indicate that inflowing water is forced by the bathymetry of the Gotland Deep to spiral anticlockwise into the deepest parts of the Gotland Deep. This produces regions of erosion in the North and West parts of the Gotland Deep, and regions of accumulation in the South and East (Emelyanov and Gritsenko, 1999). The cores 201301-5 and 20001-5, also show erosional features such as truncated laminae, which are not observed in core 201302-5. It is, therefore, plausible that the measured varve thickness of 0.7 mm represents the primary sedimentation rate in core 20001-5, but that erosion has significantly affected this core.

5. Summary

The use of SEM based techniques allows the study of lamina-scale structure of the finely laminated Littorina sediments of the Gotland Deep. Several different diatomaceous and clay-rich laminae can be distinguished, and annual lamina sequences or varves are identified. The identification of varves is a useful tool in delimiting seasonal depositional events such as the diagenetic Ca-rhodochrosite laminae which occur regularly in varves only as a winter/early spring deposit. The development and/or preservation of identifiable varves in Gotland Deep sediments is patchy and much of the record is taken up intervals of indistinctly laminated or massive sediment, that may relate to interannual–decadal variability in the extent of bottom water renewal, basin oxidation, and the destruction of varves by bioturbation.

Acknowledgements

We thank Kay Emeis of the Institute of Baltic Research, Warnemünde, Germany, who provided core material making this study possible, and Ulrick Struck also of the Institute of Baltic Research for sharing radiocarbon data. Richard Pearce is thanked for his time, advice and suggestions. Earlier manuscripts of this paper were greatly improved by comments made in review by H. Chamley, S. Björck and A. Lepland. This

research was funded by the award of NERC studentship GT4/98/ES/266 to I.T.B.

References

Alldredge, A.L., Gotschalk, C.C., 1989. Direct observation of the mass flocculation of diatom blooms: characteristics, settling velocities and formation of diatom aggregates. Deep-Sea Res. 36, 159–171.

Bergstrom, S., Carlsson, B., 1994. River runoff to the Baltic Sea, 1959–1990. Ambio 23, 280–287.

Björck, S., 1995. A review of the history of the Baltic Sea. Quat. Int. 27, 19–40.

Björck, S., Kromer, B., Johnsen, S., Bennike, O., Hammarlund, D., Lemdahl, G., Possnert, G., Rasmussen, T.L., Wohlfarth, B., Hammer, C.U., Spurk, M., 1996. Atmospheric deglacial records around the North Atlantic. Science 274, 1155–1160.

Boesen, C., Postma, D., 1988. Pyrite formation in anoxic environments of the Baltic. Am. J. Sci. 288, 575–603.

Brodie, I., Kemp, A.E.S., 1994. Variation in biogenic and detrital fluxes and formation of laminae in Late Quaternary sediments from the Peruvian coastal upwelling zone. Mar. Geol. 116, 385–398.

Bull, D., Kemp, A.E.S., 1995. Composition and origins of laminae in late Quaternary and Holocene sediments from the Santa Barbara basin. In: Kennett, J.P., Baldauf, J.G. (Eds.), Proc. ODP, Sci. Res. 146, pp. 77–87.

Christiansen, C., Kunzendorf, H., 1998. Datings and sedimentation rate estimations during GOBEX – a summary. In: Emeis, K.C., Struck, U. (Eds.), Gotland Deep Experiment (GOBEX). Status Report on Investigations Concerning Benthic Processes, Sediment Formation and Accumulation. Meereswiss. Ber., Warnemünde, 34, pp. 55–76.

Danyushevskaya, A.I., 1992. Geochemistry of organic matter in bottom sediments of the Baltic Sea. Oceanology 32, 469–475.

Dean, J.M., Kemp, A.E.S., Bull, D., Pike, J., Patterson, G., Zolitschka, B., 1999. Taking varves to bits: Scanning electron microscopy in the study of laminated sediments and varves. J. Paleolimnol. 22, 121–136.

Emeis, K.C., Neumann, T., Endler, R., Struck, U., Kunzendorf, H., Christiansen, C., 1998. Geochemical records of sediments in the Eastern Gotland Basin: products of sediment dynamics in a not-so-stagnant basin? Appl. Geochem. 13, 349–358.

Emeis, K.C., Struck, U., 1998. Gotland Deep Experiment (GOBEX). Status Report on Investigations Concerning Benthic Processes, Sediment Formation and Accumulation. Meereswiss. Ber., Warnemünde, 34.

Emelyanov, E.M., Gritsenko, V.A., 1999. On the role of near-bottom currents in the formation of bottom sediments in the Gotland Basin, the Baltic Sea. Oceanology 39, 709–718.

Gingele, F.X., Leipe, T., 1997. Clay mineral assemblages in the western Baltic Sea: recent distribution and relation to sedimentary units. Mar. Geol. 140, 97–115.

Grimm, K.A., 1992. High-resolution imaging of laminated diatomaceous sediments and their paleoceanographic significance (Quaternary, ODP Site 798, Japan Sea). Proc. ODP Sci. Res. 128, 547–557.

Grimm, K.A., Lange, C.B., Gill, A.S., 1996. Biological forcing of hemipelagic sedimentary laminae: Evidence from ODP Site 893, Santa Barbara Basin, California. J. Sediment. Res. 66, 613–624.

Guillard, R.R.L., Kilham, P., 1978. Ecology of marine planktonic diatoms. In: Werner, D. (Ed.), The Biology of Diatoms. University of California Press, Berkeley, Bot. Mon., pp. 470–483.

Hallfors, G., Niemi, A., Ackefors, H., Lassig, J., 1981. Biological oceanography. In: Viopio, A. (Ed.), The Baltic Sea. Elsevier, Amsterdam.

Heiser, U., Neumann, T., Scholten, J., Stüben, D., 2001. Recycling of manganese from anoxic sediments in stagnant deeps by seawater inflow: a study of surface sediments from the Gotland Basin, Baltic Sea. Mar. Geol. 177, 151–166.

Heiskanen, A.S., Kononen, K., 1994. Sedimentation of vernal and late summer phytoplankton communities in the coastal Baltic Sea. Arch. Hydrobiol. 131, 175–198.

Huckriede, H., Meischner, D., 1996. Origin and environment of manganese-rich sediments within black shale deeps. Geochim. Cosmochim. Acta 60, 1399–1413.

Ignatius, H., 1958. On the rate of sedimentation in the Baltic Sea. Bull. Comm. Geol. Finl. 180, 135–145.

Ignatius, H., Axberg, S., Niemistö, L., Winterhalter, B., 1981. Quaternary geology of the Baltic Sea. In: Voipio, A. (Ed.), The Baltic Sea. Elsevier, Amsterdam, pp. 54–104.

Jansson, B.O., 1989. The Baltic Sea. In: Rey, L., Alexander, V. (Eds.), 13–15 May 1995. Proceedings of the sixth conference of the Comite Arctique International, pp. 283–326.

Jonsson, P., 1992. Large-scale changes of contaminants in Baltic Sea sediments during the twentieth century. Acta Uni. Uppsala 407, 1–52.

Kabailiené, M., 1995. The Baltic Ice Lake and Yoldia Sea Stages, based on data from diatom analysis in the central, south-eastern and eastern Baltic. Quat. Int. 27, 69–72.

Kemp, A.E.S., 1996. Palaeoclimatology and Palaeoceanography from Laminated Sediments. Geol. Soc. Spec. Publ., 116.

Kemp, A.E.S., Baldauf, J.G., 1993. Vast Neogene laminated diatom mat deposits from the eastern equatorial Pacific ocean. Nature 362, 141–144.

Kemp, A.E.S., Pearce, R.B., Koizumi, I., Pike, J., Rance, S.J., 1999. The role of mat-forming diatoms in the formation of Mediterranean sapropels. Nature 398, 57–61.

Kemp, A.E.S., Pearce, R.B., Pike, J., Marshall, J.E.A., 1998. Microfabric and microcompositional studies of Pliocene and Quaternary sapropels from the eastern Mediterranean. Proc. ODP Sci. Res. 160, 349–364.

Kemp, A.E.S., Pike, J., Pearce, R.B., Lange, C.B., 2000. The 'Fall dump': a new perspective on the role of a 'shade flora' in the annual cycle of diatom production and export flux.

Deep-Sea Res. Part II – Top. Stud. Oceanogr. 47, 2129–2154.
Krinsley, D.H., Pye, K., Boggs, S., Tovey, N.K., 1998. Backscattered Scanning Electron Microscopy and Image Analysis of Sediments and Sedimentary Rocks. Cambridge University Press, Cambridge, 193 pp.
Kullenberg, G., 1981. Physical oceanography. In: Viopio, A. (Ed.), The Baltic Sea. Elsevier, Amsterdam, pp. 135–181.
Manheim, F.T., 1961. A geochemical profile in the Baltic Sea. Geochim. Cosmochim. Acta 25, 52–70.
Margalef, R., 1967. The food web in the pelagic environment. Helg. Wiss. Meeresunters. 15, 548–559.
Matthäus, W., 1990. Mixing across the primary Baltic halocline. Beitr. Meereskd. 61, 21–31.
Matthäus, W., 1995. Natural variability and human impacts reflected in long-term changes in the Baltic deep water conditions: a brief review. Dtsch. Hydrogr. Z. 47, 47–65.
Matthäus, W., Schinke, H., 1994. Mean atmospheric circulation patterns associated with major Baltic inflows. Dtsch. Hydrogr. Z. 46, 321–399.
McQuoid, M.R., Hobson, L.A., 1997. A 91-year record of seasonal and interannual variability of diatoms from laminated sediments in Saanich Inlet, British Columbia. J. Plank. Res. 19, 173–194.
Mörner, N.A., 1995. The Baltic Ice Lake–Yoldia Sea transition. Quat. Int. 27, 95–98.
Morris, R.J., Niemi, A., Niemistö, L., Poutanen, E.L., 1988. Sedimentary record of seasonal production and geochemical fluxes in a nearshore coastal embayment in the northern Baltic Sea. Finn. Mar. Res. 256, 77–94.
Neumann, T., Christiansen, C., Clasen, S., Emeis, K.C., Kunzendorf, H., 1997. Geochemical records of salt-water inflows into the deeps of the Baltic Sea. Cont. Shelf Res. 17, 95–115.
Pearce, R.B., Kemp, A.E.S., Koizumi, I., Pike, J., Cramp, A., Rowland, S.J., 1998. A laminae-scale, SEM-based study of a late Quaternary diatom-ooze sapropel from the Mediterranean ridge, Site 971. Proc. ODP Sci. Res. 160, 333–348.
Pike, J., Kemp, A.E.S., 1996a. Preparation and analysis techniques for studies of laminated sediments. In: Kemp, A.E.S. (Ed.), Palaeoclimatology and Paleoceanography from Laminated Sediments. Geol. Soc. Spec. Publ., London, pp. 37–48.
Pike, J., Kemp, A.E.S., 1996b. Records of seasonal flux in Holocene laminated sediments from the Gulf of California. In: Kemp, A.E.S. (Ed.), Palaeoclimatology and Plaeoceanography from laminated sediments. Geol. Soc. Spec. Publ., London, pp. 157–169.
Pike, J., Kemp, A.E.S., 1997. Early Holocene decadal-scale ocean variability recorded in Gulf of California laminated sediments. Paleoceanography 12, 227–238.
Rahm, L., 1988. Hydrographic properties of the eastern Gotland Basin. Beitr. Meereskd. 58, 47–58.
Raukas, A., 1995. Evolution of the Yoldia Sea in the eastern Baltic. Quat. Int. 27, 99–102.
Rines, J.E.B., Hargraves, P.E., 1988. The Chaetoceros ehrenberg (Bacillariophyceae) flora of Narrangansett Bay, Rhode Island, USA. Bibliotheca Phycologyca, 195 pp.
Round, F.E., Crawford, R.M., Mann, P.G., 1990. The Diatoms: Biology and Morphology of the Genera. Cambridge University Press, Cambridge, 747 pp.
Salonen, V.-P., Grönlund, T., Itkonen, A., Sturm, M., 1995. Geochemical record on early diagenesis of recent Baltic Sea sediments. Mar. Geol. 129, 101–109.
Sancetta, C., 1989. Spatial and temporal trends of diatom flux in the British Colombian fjords. J. Plankton Res. 11, 503–520.
Sancetta, C., 1996. Laminated diatomaceous sediments: controls on formation and strategies for analysis. Geol. Soc. Spec. Publ. 116, 17–21.
Sancetta, C., Villareal, T.A., Falkowski, P., 1991. Massive fluxes of rhizosolenid diatoms: a common occurrence? Limnol. Oceanogr. 36, 1452–1457.
Schinke, H., Matthäus, W., 1998. On the causes of major Baltic inflows: an analysis of a long time series. Cont. Shelf Res. 18, 67–97.
Sivkov, V.V., Emeis, K.C., Endler, R., Zhurov, Y., Kuleshov, A., 1998. Observations of the Nepheloid layers in the Gotland Deep (August 1994). In: Emeis, K.C., Struck, U. (Eds.), Gotland Deep Experiment (GOBEX). Status Report on Investigations Concerning Benthic Processes, Sediment Formation and Accumulation. Meereswiss. Ber., Warnemünde, 34, pp. 84–96.
Smetacek, V., 2000. Oceanography: the giant diatom dump. Nature 406, 574–575.
Sohlenius, G., 1996. The history of the Baltic proper since the Late Weichselian deglaciation as recorded in sediments. Quaternaria A 3, 34.
Sohlenius, G., Sternbeck, J., Anden, E., Westman, P., 1996. Holocene history of the Baltic Sea as recorded in a sediment core from the Gotland Deep. Mar. Geol. 134, 183–201.
Sohlenius, G., Westman, P., 1998. Salinity and redox alternations in the northwestern Baltic proper during the late Holocene. Boreas 27, 101–114.
Sternbeck, J., Sohlenius, G., 1997. Authigenic sulphide deposits and carbonate mineral formation in Holocene sediments of the Baltic Sea. Chem. Geol. 135, 55–73.
Sviridov, N.I., Sivkov, V.V., Rudenko, M.V., Trimonis, E.S., 1997. Geological evidence of bottom currents of the Gotland Basin. Oceanology 37, 838–844.
Villareal, T.A., Altabet, M.A., Culver-Rymszoa, K., 1993. Nitrogen transport by vertically migrating diatom mats in the North Pacific Ocean. Nature 363, 709–712.
Villareal, T.A., Carpenter, E.J., 1989. Nitrogen-fixation, suspension characteristics and chemical composition of rhizosolenia mats in the central North Pacific. Gyre Biol. Oceanogr. 6, 387–405.
Wastegård, S., Andrén, T., Sohlenius, G., Sandgren, P., 1995. Different phases of the Yoldia Sea in the north-western Baltic Proper. Quat. Int. 27, 121–129.
Yemelyanov, E.M., Trimonis, E.S., Lukashina, N.P., Slobodyannik, V.M., 1995. Stratigraphy and composition of the stratotype core from the Gotland Deep (Baltic Sea). Oceanology 35, 99–104.
Zenkevitch, L., 1963. Biology of the Seas of the USSR. George Allen and Unwin Ltd., London, 270 pp.